

Supplemental materials:

**Thermoacoustic Imaging and Therapy Guidance based on
Ultra-short Pulsed Microwave Pumped Thermoelastic Effect Induced
with Superparamagnetic Iron Oxide Nanoparticles**

Liewei Wen¹, Sihua Yang^{1*}, Junping Zhong¹, Quan Zhou², Da Xing^{1*}

1. MOE Key Laboratory of Laser Life Science & Institute of Laser Life Science,
College of Biophotonics, South China Normal University, Guangzhou, China

2. Medical Imaging Center, First Affiliated Hospital of Jinan University, Guangzhou,
China

* Corresponding author: Da Xing, Ph.D. E-mail: xingda@scnu.edu.cn; Sihua Yang,
Ph.D. E-mail: yangsh@scnu.edu.cn

Supplemental Materials and Methods

Materials

$\text{FeCl}_3 \cdot 6\text{H}_2\text{O}$, ethylene glycol, polyethylene glycol (PEG, $M_w=4000$), and $\text{NaAc} \cdot 3\text{H}_2\text{O}$ were purchased from Aladdin Co. Ltd. Albumin from human serum (HSA), N-hydroxysulfosuccinimide (NHS), 1-Ethyl-3-(3-dimethylaminopropyl) carbodiimide (EDC) and Fluorescein isothiocyanate (FITC) were obtained from Sigma-Aldrich Co. (MO, USA). Cell-counting kit-8 (CCK-8) was obtained from Dojindo Laboratories (Kumamoto, Japan). Annexin V-FITC/PI was purchased by Becton, Dickinson & Co. Other chemicals used in this work were all of analytical grade. All the reagents were used without further purification.

Albumin coated superparamagnetic iron oxide nanoparticles (SPIO) synthesis

Firstly, the SPIO was synthesized by the solvothermal reaction [1, 2]. $\text{FeCl}_3 \cdot 6\text{H}_2\text{O}$ (0.54 g) was dissolved in ethylene glycol (40 mL) to form a clear solution. Then $\text{NaAc} \cdot 3\text{H}_2\text{O}$ (1.44 g) and PEG-4000 (0.4 g) were added and vigorously stirred to completely dissolve then, sealed the mixture solution in a teflonlined stainless-steel autoclave (50 mL capacity). Hydrothermal reactions were conducted at $200\text{ }^\circ\text{C}$ for 8 h. After the reaction was carried out, the black sample was collected with the help of an external magnetic field and then rinsed with alcohol and distilled water several times. The next, SPIO functionalized with HSA according to the amide reaction reported previously [3-5]. In briefly, 100 mg SPIO were dispersed in 100 mL PBS, 12 mg EDC and 6 mg NHS were added to reacting for 12 hours. Then 100 mL HSA (1mg mL^{-1} in PBS) solution was added and sonicated for 2 hours, the mixture continued reacting for

16 hours. The final product (HSA- SPIO) was collected with the help of an external magnetic field and rinsed with PBS several times.

Characterization experiments

The morphology and size of SPIO and HSA-SPIO were examined by JEM-100CXII transmission electron microscope (TEM) with voltage of 100 kV and current of 70 pA. Size distribution and surface potential of the particles was detected by a Malvern Zetasizer Nano ZS90 instrument (Malvern, UK). Infrared (IR) spectra were recorded in the wavenumbers ranging from 4000 to 500 cm^{-1} with a Nicolet model 759 Fourier transform infrared (FT-IR) spectrometer using a KBr wafer.

Microwave pumped TA signal and imaging

The procedure of TA signal detection referred to the previous report [6, 7]. Briefly, microwave generator with a central frequency of 434 MHz was adjusted to transmit the ultra-short microwave with pulsed the peak power of 10 MW, repetition frequency of 10 Hz and pulse duration of 10 ns. The microwave pumped by an antenna, which its effective radiation area was about 1000 cm^2 . The energy density per pulse was about 100 $\mu\text{J cm}^{-2}$. A focused ultrasonic transducer (I10P6NF20, DOPPLER, China) with a central frequency of 10 MHz (100% bandwidth at 6 dB), a focal length of 20 mm, and an active element of 6 mm in diameter was employed to detect the TA signals. Deionized water and HSA-SPIO with SPIO concentrations of 0.0625, 0.125, 0.25, 0.5 and 1 mg mL^{-1} were injected into a silicon tube to detect their microwave-induced TA signals.

The schematic of TA imaging was presented in Scheme 1B. TA imaging system of

HSA-SPIO solution and tumor-bearing mice was designed according to Ye et al [8]. A full ring transducer (10C384-1.62×8-R100 AHA001, Doppler Ltd., China) consisting of 384 detectors was applied to acquire the TA signal. The central frequency of the transducer is 10 MHz and the bandwidth ranges from 64.5% to 92.4%. In the imaging process, the tumor-bearing mice were anesthetized and the dorsal tumors of mice were immersed in mineral oil. When the microwave pulse irradiated the tumor region, the TA signal was detected by the 384 detectors simultaneously, then transmitted to a homemade 64-channel data acquisition system (DAS) in sequence with a homemade 384-64 channel switching system. Finally, the 384-channel signals are used to reconstruct a 2-D image via a filtered back-projection algorithm.

Magnetic properties of HSA-SPIO and MRI performance

The magnetic properties of HSA-SPIO were measured on a vibrating sample magnetometer (VSM) at room temperature. For *in vitro* MRI, different concentration HSA-SPIO were filled in Eppendorf tubes and then embedded in an agar phantom. MRI was performed with a 1.5 T Imager (GE Signa HD, 1.5 T MR, GE Healthcare, Milwaukee, WI, USA). MR coronal images were scanned using a fast spin echo T₂ sequence (repetition time (ms)/echo time (ms)=4000/108, 16 echo train length) and a spin-echo T₁ sequence (repetition time (ms)/echo time (ms)=500/17.9). Images were obtained with a matrix size of 256×256. Two measurements were acquired at the section thickness of 2 mm and field view of 13×13 cm². The region of interest (ROI) for signal intensity measurement was 26 mm². The ROIs were randomly selected and measured in each tube. The specific relaxivity values of R were calculated through the

curve fitting of $1/T_2$ (s^{-1}) vs. the Fe concentration (mM) as the slope of the resulting linear plot. MRI of tumor-bearing mice was conducted on a 1.5-T clinical MRI scanner equipped with a special coil designed for small animal imaging.

Cell-like microcapsules preparation

The alginate-polylysine-alginate microcapsules as cell-like models were prepared according to the previous report [9]. Firstly, HSA-SPIO (5 mg) was added in 5 mL sodium alginate solution (1.5% w/w) containing a lipophilic surfactant (Span 85, 2.0% w/w) and stir for 15 min. Then, 15 mL of 0.1 M $CaCl_2$ solution was added to form Ca-alginate microspheres and the emulsion continued to stir for 1 h. Ca-alginate microspheres were collected and suspended in a solution of polylysine (0.1% w/w) for 10 min. The precipitate washed with deionized water and then immersed in alginate solution (0.05% w/w) for 10 min. Finally, the microcapsules containing HSA-SPIO were immersed in sodium citrate solution (0.05 M) for 6 min, washed with deionized water and stored at 4 °C for further experiment.

Cell culture

4T1 cell maintained in RPMI-1640 Medium (GIBCO), supplemented with 10% FBS (Hyclone) at 37 °C in a humidified atmosphere of 5% CO_2 . The cell culture media were supplemented with 100 units mL^{-1} penicillin and 100 $g mL^{-1}$ streptomycin.

Animal models

For the subcutaneous tumor model, 4T1 cells (1×10^6) in serum-free RMPI-1640 medium (100 μL) were subcutaneously injected into the flank region of female Balb/c mice (6-8 weeks). Seven days after tumor inoculation, the tumor volume reached

50-60 mm³. On the other hand, the orthotopic tumor models were developed as previous reports [10], 50 μL of the cell suspension (1×10⁶) was injected into the mammary fat pad inferior to the nipple. The breast tumor grew on the mammary fat pad of mice, keeping a distance from the surface skin.

Hemolysis test

Different concentration HSA-SPIO was used for evaluating the hemolysis *in vitro*. Red blood cell (RBC) was isolated from 2 mL fresh EDTA-stabilized rabbit's heart blood by centrifugation and washed with phosphate saline-buffered solution (PBS). Then the RBC was dispersed in 10 mL PBS solution. Different concentration of HSA-SPIO (0.0625, 0.125, 0.25, 0.5, 1, 2 mg mL⁻¹) in 1 mL RBC solution was cultured at temperature for 3 h. The PBS solution was used as negative control (0% lysis) and deionized water was used as positive control (100% lysis) respectively. Each group involved three parallel experiments in duplicate to minimize statistical error. After incubation, these mixtures were centrifuged by 10000 rpm for 3 min, and the supernatant was measure the absorbance of 570 nm by UV-Vis spectrophotometer. The hemolysis ratio (HR%) was calculated as followed: $HR\% = \frac{\text{tested sample} - \text{negative control}}{\text{positive control} - \text{negative control}} \times 100$.

***In vitro* cellular uptake of HSA-SPIO and TA shockwave induced cell membrane destruction**

To evaluate the ability of HSA-SPIO binding to 4T1 cells, HSA-SPIO was labeled with fluorescein isothiocyanate (FITC) to form FITC-HSA-SPIO. 4T1 cells were seeded in 35 mm glass bottomed dishes and cultured for 24 h. After incubated with

FITC-HSA-SPIO for 1h, 2h, medium was removed, and cells were washed with PBS for 3 times. These cells were imaged by a commercial laser scanning microscope (LSM510/ConfoCor2) combination system (Zeiss, Germany) equipped with a Plan-Neo fluar 40×/1.3 NA oil DIC objective. The nano-probe was excited at 488 nm with an Ar-ion laser (reflected by a beam splitter HFT 488 nm) and the fluorescence emission was recorded through a 500-550 nm IR band-pass filter.

To investigate the capability of TA shockwave induced cell membrane destruction, 4T1 cells were incubated with HSA-SPIO for 2 hours, then propidium iodide (PI) was added and immediately irradiated with ultra-short pulsed microwave for 5 min (peak power of 40 MW, repetition frequency of 10 Hz, energy density per pulse was about $400 \mu\text{J cm}^{-2}$). PI was excited at 488 nm with an Ar-ion laser (reflected by a beam splitter HFT 488 nm) and the fluorescence emission was recorded through a 560 nm LP emission filter.

Cytotoxicity assays

To detect TA cytotoxicity, tumor cells incubated with HSA-SPIO for 2 h, then irradiated by the 434 MHz pulsed microwave with the peak power of 40 MW ($400 \mu\text{J cm}^{-2}$ per pulse) and pulse repetition frequencies of 10 Hz for 5 min. Cell cytotoxicity was assessed with CCK-8 at 24 h after microwave irradiation.

To analyze the cellular apoptosis on the nuclear morphology after different treatment, cells were seeded in 35 mm glass bottomed dishes and incubated with HSA-SPIO (0.2 mg mL^{-1}) for 2 h, then irradiated by the microwave for 5 min. Six hours after treatment, the cells were stained with Hoechst 33258 for 10 min at room temperature

and washed three times with PBS. The cell samples were excited by a light source with a 330-380 nm band-pass filter, and emitted light was detected through a 450-490 nm band-pass filter. On the other hand, statistical analysis of cell apoptosis was in accordance with annexin V-FITC/PI stain, and detected by flow cytometry. The fluorescence emission of FITC was measured at 515-545 nm and that of DNA-PI complexes at 564-606 nm.

***In vivo* TA therapy**

The tumor-bearing mice were randomly divided into four groups (n=7 per group). The control group was only intravenously injected with 0.1 mL PBS. In the microwave treatment group, mice were covered with metallized knitted net fabrics except for tumor region then irradiated with microwave for 5 min (peak power of 40 MW, repetition frequency of 10 Hz, energy density per pulse was about $400 \mu\text{J cm}^{-2}$). The HSA-SPIO treatment group was intravenously injected with HSA-SPIO (8 mg mL^{-1} 0.1 mL) only. And the mice of HSA-SPIO+Microwave group were intravenously injected with HSA-SPIO (8 mg mL^{-1} 0.1 mL), 4 hours later, mice body was covered with metallized knitted net fabrics except for tumor region and irradiated with microwave for 5 minutes. The tumor sizes and body weights of mice were measured every three days and calculated the volume, and tumor volume was calculated using the following equation: $\text{tumor volume} = \frac{A \times B^2}{2}$, which A is the maximum diameter of tumor and B is the minimum diameter of tumor. Relative tumor volumes were calculated as V / V_0 (V_0 is the tumor volume when the treatment was initiated). After therapy, major organs as well as tumors were collected and sectioned to $8 \mu\text{m}$ slices

for H&E staining.

Tissue slicing and staining

To detect the distribution of HSA-SPIO, Prussian-blue staining was used for identifying the presence of iron. In briefly, the tumor-bearing mice were i.v. injected with HSA-SPIO and sacrificed at 4 h post injection. Major organs from these mice were collected, fixed in 10% neutral buffered formalin, processed routinely into paraffin, sectioned at 8 μ m, stained with Prussian-blue, and examined by a digital microscope. Examined tissues included heart, liver, spleen, lung, kidney, and tumor.

Histological assessment of tumor samples after different treatment was performed by hematoxylin and eosin (H&E) and terminal deoxynucleotidyl transferase dUTP nick end labeling (TUNEL) staining. Mice in the above four groups was sacrificed at 48 h after different treatment to analyzing the morphological changes resulting from TA therapy in the tumor section. Twenty-one days later, mouse major organs from the four groups were collected and stained by H&E according to the standard techniques to evaluating the toxicity.

Supplemental figures

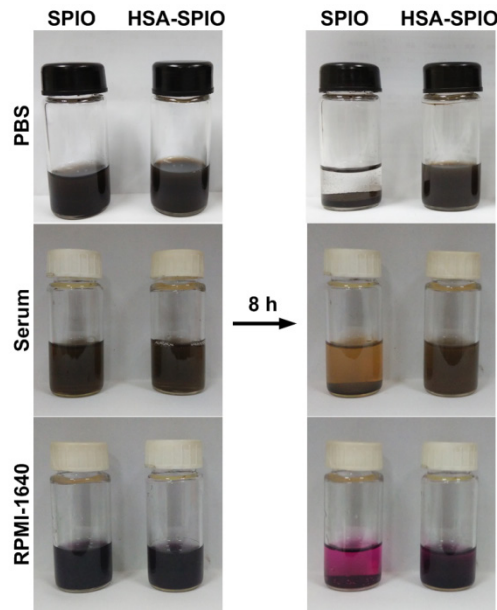


Figure S1. The stability of SPIO and HSA-SPIO in PBS, serum and RPMI-1640 during the 8 hours.

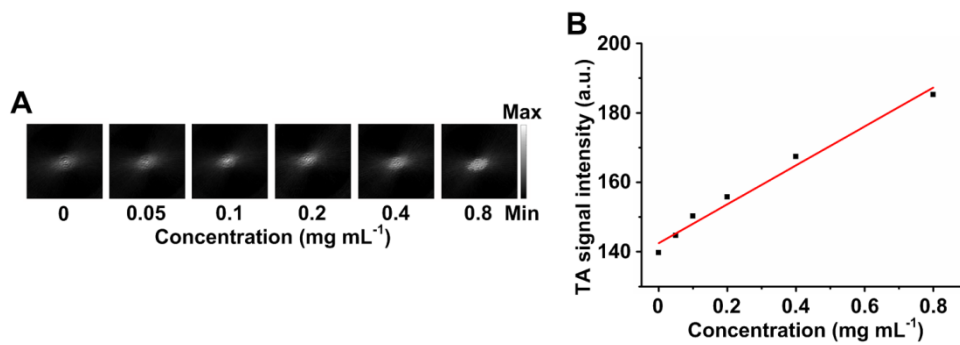


Figure S2. TA images of HSA-SPIO dispersing in PBS. (A) TA tomography imaging of HSA-SPIO. (B) Linear fit of TA signal intensity.

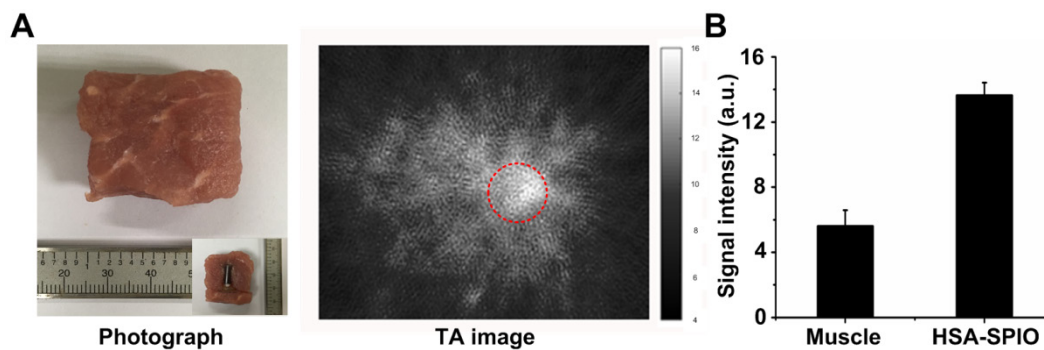


Figure S3. TA imaging for HSA-SPIO embedded inside tissue. (A) Photograph of the phantom and TA image obtained using a full ring transducer consisting of 384 detectors. The red dotted circle indicated where the HSA-SPIO solution was embedded inside.

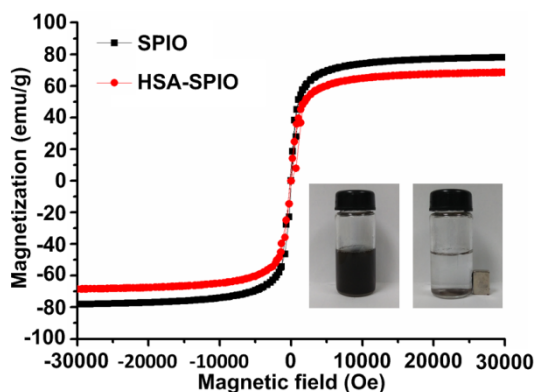


Figure S4. Magnetization loops of SPIO and HSA-SPIO. Inset is the photograph of HSA-SPIO with magnet and without magnet.

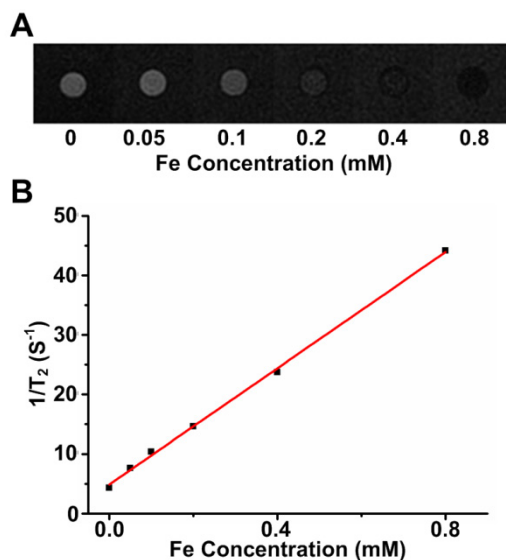


Figure S5. MR property of HSA-SPIO. (A) T_2 -weighted MR images of HSA-SPIO aqueous solutions with different concentrations (1.5 T). (B) T_2 relaxation rates with iron concentration (mM) of HSA-SPIO particles in aqueous solution.

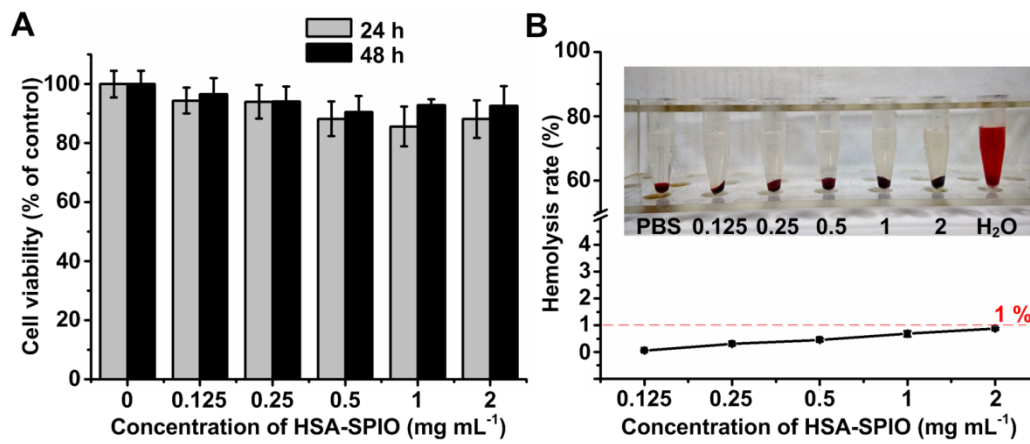


Figure S6. Toxicity evaluation of the HSA-SPIO. (A) Cell viability under different concentration HSA-SPIO was detected at 24 h and 48 h after incubation. (B) *In vitro* hemolysis test. Hemolysis ratio of HSA-SPIO with different concentrations, inset represents the hemolysis images the tubes, PBS as negative control group and water as positive control group (n=3 in each treatment group).

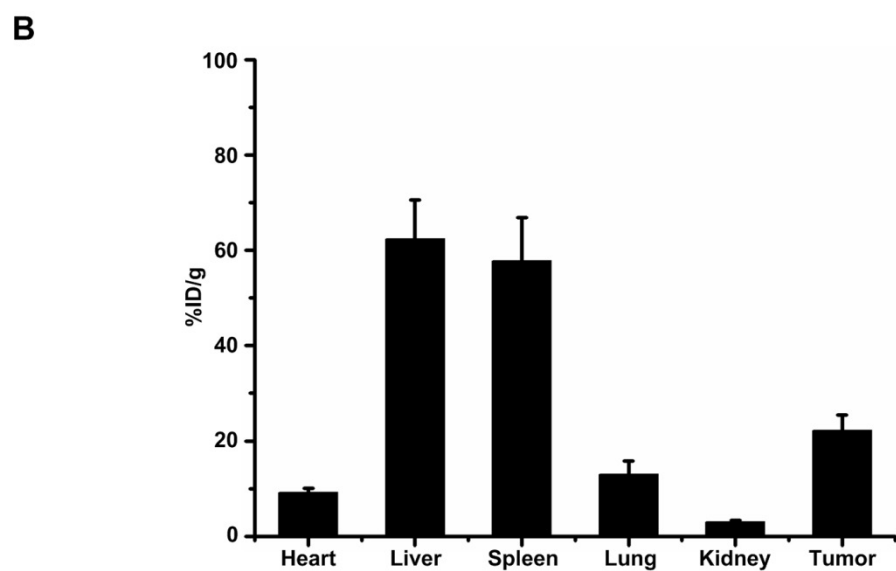
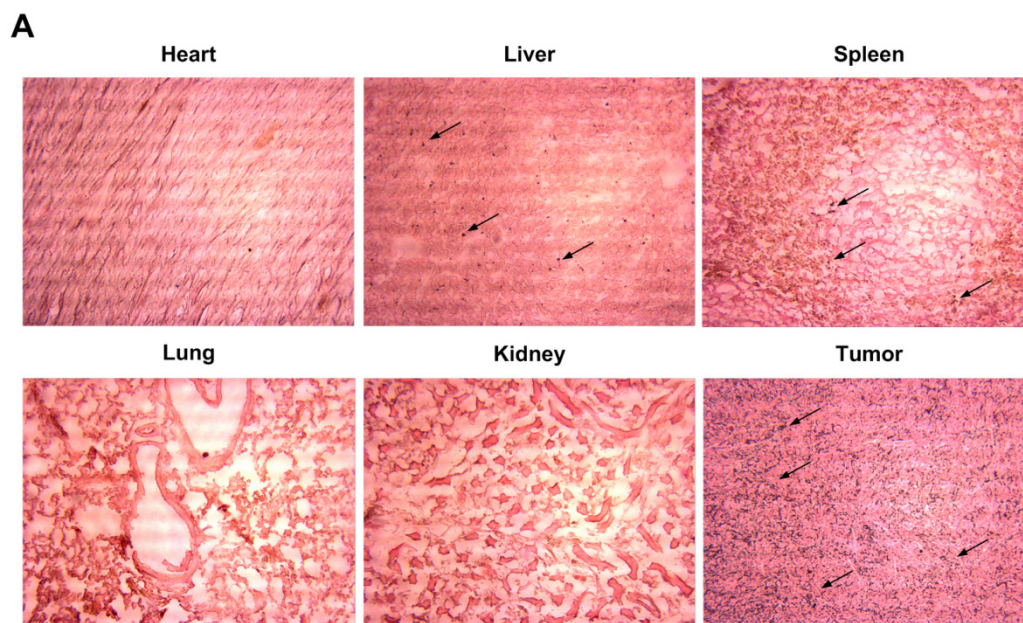


Figure S7. Biodistribution of HSA-SPIO in 4T1 tumor-bearing mice. (A) Prussian-blue stained tissue slices of major organs and tumor collected 4 h after i.v. injected with HSA-SPIO. (B) The amounts of Fe in the tissues were analyzed by ICP-MS. Error bars are standard errors with $n = 3$.

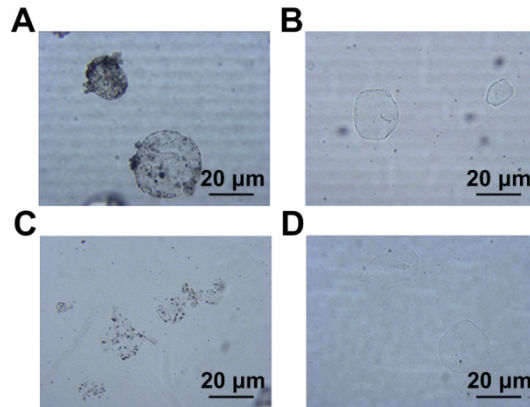


Figure S8. Destruction effect of TA shockwave for cell-like model. (A) Cell-like microcapsules with HSA-SPIO inside and (B) microcapsules without HSA-SPIO before microwave irradiation. (C) The microcapsules with HSA-SPIO inside were broken after microwave irradiation. (D) Microcapsules without HSA-SPIO retained good morphology after microwave irradiation.

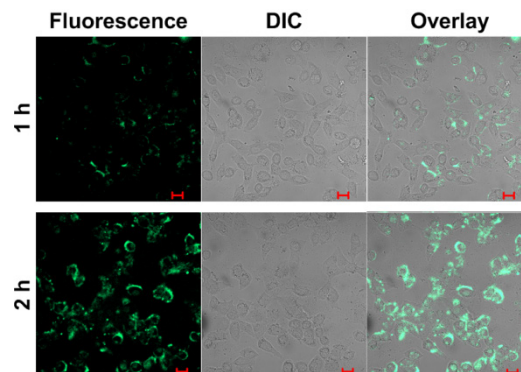


Figure S9. *In vitro* cellular uptake of HSA-SPIO. Cells were incubated with FITC-HSA-SPIO for 1 and 2 h. Scale bar was 20 μm .

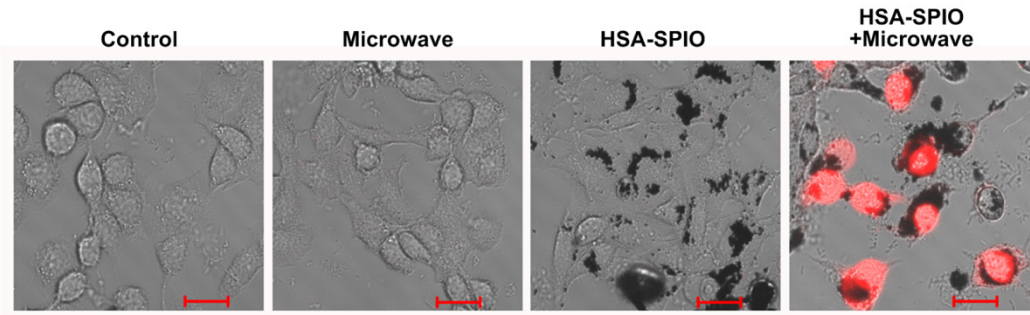


Figure S10. TA shockwave induced cell membrane destruction. 4T1 cells incubated with HSA-SPIO for 2 hours, PI was added and immediately irradiated with microwave for 5 min. Scale bar was 20 μm .

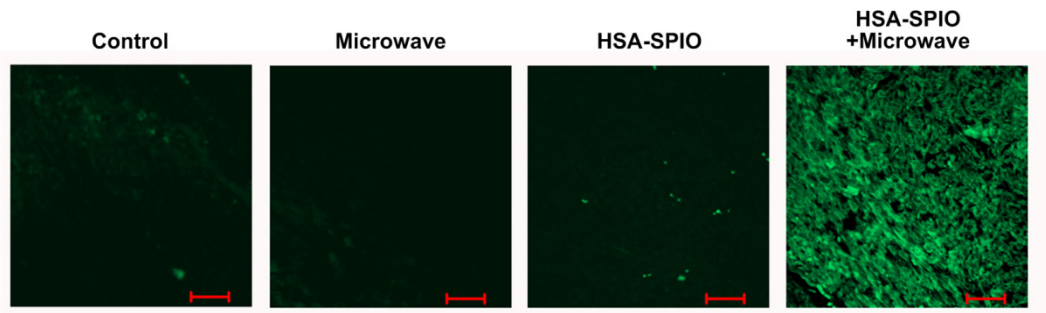


Figure S11. Tissue slices of the different treatment with TUNEL staining to analyze the cancer cell apoptosis. Scale bar was 50 μm .

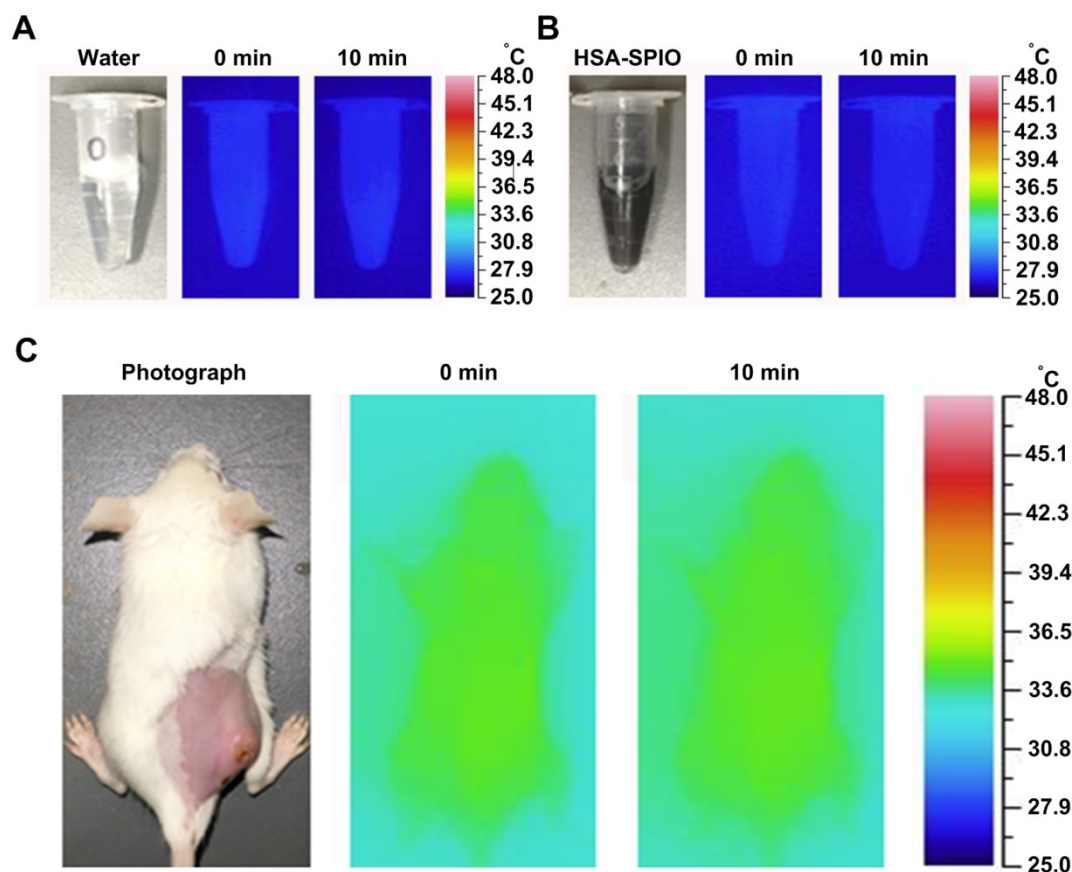


Figure S12. Infrared thermal imaging pictures of solution and tumor-bearing mice. (A) Thermographic images of deionized water and (B) HSA-SPIO solution recorded before and after microwave irradiation for 10 min. (C) Thermographic images of the HSA-SPIO+Microwave group acquired at pre- and post-microwave irradiation.

References

1. Deng H, Li XL, Peng Q, Wang X, Chen JP, Li YD. Monodisperse magnetic single-crystal ferrite microspheres. *Angew Chem Int Ed Engl.* 2005; 44: 2782-5.
2. Liu J, Sun ZK, Deng YH, Zou Y, Li CY, Guo XH, et al. Highly Water-Dispersible Biocompatible Magnetite Particles with Low Cytotoxicity Stabilized by Citrate Groups. *Angew Chem Int Ed Engl.* 2009; 48: 5875-9.
3. Ahmad MW, Kim CR, Baek JS, Chang Y, Kim TJ, Bae JE, et al. Bovine serum albumin (BSA) and cleaved-BSA conjugated ultrasmall Gd_2O_3 nanoparticles: Synthesis, characterization, and application to MRI contrast agents. *Colloids Surf.* 2014; 450: 67-75.
4. Chen Q, Wang C, Cheng L, He WW, Cheng Z, Liu Z. Protein modified upconversion nanoparticles for imaging-guided combined photothermal and photodynamic therapy. *Biomaterials.*

2014; 35: 2915-23.

5. Shen S, Kong FF, Guo XM, Wu L, Shen HJ, Xie M, et al. CMCTS stabilized Fe₃O₄ particles with extremely low toxicity as highly efficient near-infrared photothermal agents for in vivo tumor ablation. *Nanoscale*. 2013; 5: 8056-66.
6. Lou CG, Yang SH, Ji Z, Chen Q, Xing D. Ultrashort Microwave-Induced Thermoacoustic Imaging: A Breakthrough in Excitation Efficiency and Spatial Resolution. *Phys Rev Lett*. 2012; 109.
7. Wen LW, Ding WZ, Yang SH, Xing D. Microwave pumped high-efficient thermoacoustic tumor therapy with single wall carbon nanotubes. *Biomaterials*. 2016; 75: 163-73.
8. Ye FH, Ji Z, Ding WZ, Lou CG, Yang SH, Xing D. Ultrashort Microwave-Pumped Real-Time Thermoacoustic Breast Tumor Imaging System. *IEEE Trans Med Imaging*. 2016; 35: 839-44.
9. Wen L, Ding W, Yang S, Xing D. Microwave pumped high-efficient thermoacoustic tumor therapy with single wall carbon nanotubes. *Biomaterials*. 2016; 75: 163-73.
10. Sheng ZH, Hu DH, Zheng MB, Zhao PF, Liu HL, Gao DY, et al. Smart Human Serum Albumin-Indocyanine Green Nanoparticles Generated by Programmed Assembly for Dual-Modal Imaging-Guided Cancer Synergistic Phototherapy. *ACS Nano*. 2014; 8: 12310-22.